Research Square

Preprints are preliminary reports that have not undergone peer review.
They should not be considered conclusive, used to inform clinical practice,
or referenced by the media as validated information.

# Prenatal Stress Is Associated With a Sex-Specific Camkii Modulation in Aged Mouse Prefrontal Cortex

**Bruno Calsa**
Universidade Estadual de Campinas (UNICAMP)
**Amanda Cristina de Souza**
Universidade Estadual de Campinas (UNICAMP)
**Luiz Marcos Frediani Portela**
Universidade Estadual de Campinas (UNICAMP)
**Gabriel Boer Grigoletti-Lima**
Universidade Estadual de Campinas (UNICAMP)
**José Antônio Rocha Gontijo**
Universidade Estadual de Campinas (UNICAMP)
**Patrícia Aline Boer**
boer@unicamp.br

Universidade Estadual de Campinas (UNICAMP)

**Research Article**

**Keywords:** prenatal stress, prefrontal cortex, proteomics, CaMKII, sex differences, brain aging, developmental origins of health and disease

**Posted Date:** November 11th, 2026

**DOI:** https://doi.org/10.21203/rs.3.rs-11472287/v1

**License:** This work is licensed under a Creative Commons Attribution 4.0 International License.
Read Full License

**Additional Declarations:**
No competing interests reported.

Tables are available in the Supplementary Files section.

# PRENATAL STRESS IS ASSOCIATED WITH A SEX-SPECIFIC CAMKII MODULATION IN AGED MOUSE PREFRONTAL CORTEX

Bruno Calsa[1], Amanda Cristina de Souza[1], Luiz Marcos Frediani Portela[2], Gabriel Boer Grigoletti-Lima[1], José Antônio Rocha Gontijo[1,3], Patrícia Aline Boer[1,3*]

[1]Fetal Programming and Hydroelectrolyte Metabolism Laboratory, Department of Internal Medicine, School of Medical Sciences, State University of Campinas (UNICAMP), Campinas, SP, Brazil.

[2] Department of Structural and Functional Biology, State University of Campinas, Campinas, SP, Brazil.

[3]National Institute of Science and Technology in Developmental Origins of Health and Disease (INCT-DOHaD Brasil), Campinas, SP, Brazil.

***Corresponding author**

Patricia Aline Boer, Ph.D.

Fetal Programming and Hydroelectrolyte Metabolism Laboratory, Department of Internal Medicine, Faculty of Medical Sciences Organization Campinas State University (UNICAMP), Rua Cinco de Junho, 350, Cidade Universitária Zeferino Vaz, Campinas, SP, 13087-051, Brazil. boer@unicamp.br

**Acknowledgments.** We thank the facility Mass Spectrometry Laboratory (MAS) of the Brazilian Biosciences National Laboratory (LNBio), Brazilian Center for Research in Energy and Materials (CNPEM), under proposal number 20242650.

# PRENATAL STRESS IS ASSOCIATED WITH A SEX-SPECIFIC CAMKII MODULATION IN AGED MOUSE PREFRONTAL CORTEX


## ABSTRACT

Animal evidence has suggested that prenatal stress programs sex-specific trajectories of brain aging; however, the molecular correlates of these trajectories in the aged prefrontal cortex (PFC) have remained undisclosed. Previous report shows that unpredictable chronic mild stress (UCMS) applied to C57BL/6J dams during gestation, followed by fragmented maternal care, produced in male offspring a progression from midlife anhedonia to hyperlocomotion, reduced avoidance and spatial memory deficits at 18 months, whereas female offspring developed late-onset anhedonia with preserved hippocampus-dependent memory. Herein, proteomic LC-MS/MS was used to investigate the prefrontal cortex (PFC) of 18-month-old C57BL/6J offspring exposed to UCMS protocol. CaMKIIα and CaMKIIβ showed opposite stress-associated changes between sexes. An exploratory postsynaptic module comprising CaMKII isoforms and IQSEC1/2 increased in females and decreased in males, with a significant sex-by-stress interaction, corroborated by Western blotting. In males, mitochondrial aspartate aminotransferase (GOT2) was the most robust individual change, accompanied by increased phosphorylated tau and AKT. Females exhibited increased CaMKII abundance alongside reduced phosphorylation ratios and additional neuropeptidergic, bioenergetic, and neuroimmune candidates. These findings suggest sex-dependent molecular adaptations in the aged PFC following prenatal stress.



**Keywords:** prenatal stress; prefrontal cortex; proteomics; CaMKII; sex differences; brain aging; developmental origins of health and disease.

## INTRODUCTION

The Developmental Origins of Health and Disease (DOHaD) concept posits that adverse conditions during gestation program the structure and function of the offspring organs, increasing the risk of chronic disease throughout life. Considering the brain, excessive exposure to maternal glucocorticoids during critical windows of neurogenesis and synaptogenesis has been associated with persistent alterations of the hypothalamic-pituitary-adrenal (HPA) axis, of monoaminergic circuits and of the prefrontal-limbic network that regulates emotion, motivation and executive control [1, 2]. Notably, these effects are sex-dependent: male fetuses appear more vulnerable to placental and glucocorticoid insults, and prenatal stress has been reported to increase anxiety-like and depression-like behavior predominantly in male offspring [3–6], whereas stress-induced cognitive changes in females are more variable and frequently opposite to those of males [7–9]. Moreover, the placenta responds to maternal adversity in a sex-specific manner [10, 11], the postnatal environment may amplify or attenuate the prenatal insult, as shown by cross-fostering experiments [12], and fragmented and unpredictable maternal care is per se a programming signal for emotional circuits [13, 14]. Importantly, outcomes are heterogeneous, since only a fraction of prenatally stressed offspring develop pathology while the remaining animals are resilient [15].

Most studies addressing prenatal stress, however, have evaluated adolescent or young adult offspring, and the late consequences of this insult, when the prenatal programming interacts with the biology of aging, remain poorly characterized. The few longitudinal data available indicate that prenatal stress accelerates the age-related dysfunction of the HPA axis and the emergence of cognitive impairments [16], and recent work has emphasized that the developmental timing of adversity, rather than its nature, determines long-term trajectories [17]. In our unpublished study [18], we applied an unpredictable chronic mild stress (UCMS) protocol to C57BL/6J dams during gestation and followed male and female offspring until 18 months of age. Stressed dams displayed

fragmented and less predictable maternal behavior, and the offspring of both sexes were born with lower body weight and showed postnatal catch-up growth. Male offspring presented anhedonia at 12 months, which progressed at 18 months to hyperlocomotion, increased rearing and jumping, reduced open-arm avoidance in the elevated plus maze and persistent spatial memory and search-strategy deficits in the Barnes maze. In contrast, female offspring showed hypoactivity and reduced anxiety-like behavior at 12 months and late-onset anhedonia at 18 months, while recognition and spatial memory were preserved or even enhanced. Thus, we proposed that prenatal stress accelerates fronto-striatal decline in males and promotes a transient, costly reallocation of neural resources in females. Nevertheless, that interpretation was built exclusively on behavioral evidence, and protein-level analyses were explicitly pointed out as necessary to validate the proposed mechanisms.

The prefrontal cortex (PFC) is a natural candidate for such an analysis. It is one of the regions most sensitive to glucocorticoids and to aging, its pyramidal neurons undergo stress-induced dendritic and spine remodeling, and it exerts top-down control over the striatum, the amygdala and the hippocampus [19–21]. Additionally, the PFC response to stress is sexually dimorphic: chronic stress retracts apical dendrites of medial PFC neurons in male rats, whereas it increases apical dendritic length in females through an estradiol-dependent mechanism [22, 23], and prenatal stress reduces spine density and dendritic complexity in the anterior cingulate and orbitofrontal cortices of male offspring[24]. Proteomic studies of the PFC after prenatal or chronic stress have been conducted mainly in young adult male rats, with labeling-based or gel-based approaches [25, 26] and, to the best of our knowledge, no study has described the PFC proteome of aged male and female offspring exposed to prenatal stress.

Taking into account the above data, the current study was conducted to search whether prenatal UCMS is associated with sex-specific alterations of the PFC proteome of 18-month-old offspring, and whether these alterations are congruent with the sexually divergent behavioral trajectories described in the companion study. We hypothesized that: (a) prenatal stress modifies the aged PFC proteome in a sex-dependent manner; (b) the male proteome would reveal a reduction of synaptic plasticity machinery consistent with fronto-striatal decline; and (c) the female proteome would reveal changes in reward-related and metabolic pathways consistent with late-onset anhedonia. To this end, we combined data-independent acquisition (DIA) mass spectrometry, an animal-level statistical re-analysis with a formal sex-by-stress interaction test, functional enrichment, cell-type mapping and Western blot, and we integrated these data with the behavioral phenotype at the group level, explicitly confronting favorable, unfavorable and divergent evidence from the literature.

## MATERIALS AND METHODS

### *Ethical statement and animals*

All experimental procedures were conducted in accordance with the guidelines of the Brazilian National Council for the Control of Animal Experimentation (CONCEA) and were approved by the Ethics Committee for Animal Research of the State University of Campinas (CEUA: 5774-1/2021), and the study is reported according to the ARRIVE 2.0 guidelines. C57BL/6J mice were obtained from the Multidisciplinary Center for Biological Research (CEMIB/UNICAMP) and maintained at 21 ± 2 °C under a 12:12 h light-dark cycle, with water and standard chow *ad libitum*.

### *Prenatal unpredictable chronic mild stress*

Pregnant dams were randomly assigned to the control (C) or stress (S) group. The S group was subjected to a UCMS protocol in which a single stressor was applied per day, in a semi-random

rotating sequence to prevent habituation: lights on during the dark phase (12 h), cage without bedding (3 h), cage tilted at 45° (7 h), food restriction (24 h), water restriction (24 h), wet cage (200 mL of water in the bedding, 8 h), white noise (1500 Hz, 92 dB, 1 h), cage shaking (30 min), restraint during 4 h and forced swim in water at 31 °C (1 h). Control dams were maintained under standard housing, with routine cage changes at the same time of day [18].

After weaning, the offspring were housed by sex and at 18 months of age the animals were deeply anesthetized with isoflurane by inhalation and, after confirmation of the absence of the pedal withdrawal reflex, euthanized by decapitation. The PFC was dissected in seven female (4 C and 3 S) and six male (3 C and 3 S) offspring and proteomic analyses were conducted. N = one animal from different dam.

*Sample preparation for LC-MS/MS*

PFC samples were homogenized in 8 M urea, 75 mM NaCl, 50 mM Tris pH 8.2, Halt Protease Inhibitor Cocktail (Thermo Scientific, Cat. No. 87786), and incubated at room temperature for 30 min under agitation. Subsequently, samples were centrifuged at 12,000 × g for 30 min at 4 °C, and the supernatant was quantified using the BCA method. Protein samples [27] (50 µg) were subjected to denatured with an equal volume of 8 M urea and reduced with dithiothreitol (DTT) to a final concentration of 5 mM for 25 min at 56 °C. Cysteine residues were subsequently alkylated with iodoacetamide (IAA; 14 mM final concentration) for 30 min at room temperature, protected from light. The urea concentration was reduced to approximately 1.6 M by dilution with 50 mM ammonium bicarbonate. Calcium chloride was added to a final concentration of 1 mM, and proteins were digested with sequencing-grade modified trypsin at an enzyme-to-substrate ratio of 1:50 (w/w) for 16 h at 37 °C. Digestion was stopped by adding trifluoroacetic acid (TFA) to a final

concentration of 0.4%. Samples were centrifuged at 2,500 × g for 10 min at room temperature, and the supernatants were collected. Peptides were desalted using C18 StageTips. The tips were sequentially conditioned with methanol, 80% acetonitrile containing 1% formic acid, and 1% formic acid. Samples were acidified with 1% formic acid (pH ≤ 3), loaded onto the conditioned tips, and washed with 1% formic acid. Peptides were eluted with 80% acetonitrile containing 1% formic acid. The eluates were dried by lyophilization and stored at −20 °C until LC–MS/MS analysis.

*LC-MS/MS analysis*

Mass spectrometry analyses were performed at the Mass Spectrometry Laboratory (MAS) of the Brazilian Biosciences National Laboratory (LNBio), Brazilian Center for Research in Energy and Materials (CNPEM), under proposal number 20242650. Peptides were analyzed in an Orbitrap Exploris 240 mass spectrometer (Thermo Fisher Scientific, USA) coupled to an Evosep One liquid chromatography system (Evosep, Odense, Denmark) through a nanoelectrospray ion source, in DIA mode. Peptides were preconcentrated on EV2001 C18 Evotips and separated on an Aurora Elite XT C18 UHPLC column (IonOpticks, Australia) (15 cm × 75 µm, 1.7 µm particle size) with the Evosep Whisper Zoom 20 samples-per-day method. The nanoelectrospray voltage was 1.7 kV and the source temperature 275 °C. Full MS scans were acquired at a resolution of 120,000 over m/z 350-1400, with an automatic gain control (AGC) target of 300% and maximum injection time of 45 ms. MS/MS scans were acquired with 34 isolation windows of 20 m/z from 361 to 1033 m/z, AGC target of 1000%, normalized collision energy of 27% and resolution of 15,000 (Bekker-Jensen et al., 2020). All 13 samples were acquired on a single day in one sequence, in which female and male, control and stressed samples were interleaved and separated by water blank injections.

*Data processing and candidates' selection*

DIA raw files were processed in Spectronaut version 19 (Biognosys, Zurich, Switzerland) with a directDIA workflow against the *Mus musculus* UniProt reference database (21,803 entries, downloaded in July 2025), using BGS factory settings with method evaluation [28]. Trypsin/P specific peptides of 7 to 52 amino acids with up to two missed cleavages and five modifications were considered; methionine oxidation and protein N-terminal acetylation were set as variable modifications and cysteine carbamidomethylation as fixed modification. Identification thresholds were precursor Q value < 0.01, precursor PEP < 0.2, protein Q value (experiment) < 0.01, protein Q value (run) < 0.05 and protein PEP < 0.75. Label-free quantification was performed at the MS2 level with cross-run normalization, MaxLFQ protein roll-up (Cox et al., 2014) and no imputation. Female and male datasets were searched in separate Spectronaut analyses. Candidate proteins were selected by the Spectronaut differential abundance module (unpaired t-test) as protein groups with $P < 0.05$ and $|\log_2 \text{ratio}| >= 0.58$ (1.5-fold), and Storey Q values were reported [29]

*Functional enrichment, interaction networks and cell-type mapping*

Up-regulated and down-regulated candidates were analyzed separately by over-representation analysis in R (version 4.5.0). Gene symbols were mapped with org.Mm.eg.db, and Gene Ontology enrichment was performed with clusterProfiler [30], with redundancy reduction by the simplify function (similarity cut-off 0.7). KEGG pathways were analyzed with clusterProfiler and Reactome pathways with ReactomePA [31], after conversion to Entrez identifiers; terms with $P < 0.05$ were retained. Selected Gene Ontology terms and their candidates were represented as term-protein membership matrices. To provide cellular context, candidates of interest were examined

in the single-nucleus RNA-sequencing dataset SCP2126 of the Broad Institute Single Cell Portal, which comprises mouse and cynomolgus macaque cortex, thalamus and cerebellum [32].

*Western blot*

PFC were homogenized using Polytron in lysis buffer containing EDTA 10 mM, Trizma base 100 mM, sodium pyrophosphate 10 nM, sodium fluoride 100 mM, sodium orthovanadate, phenylmethylsulfonyl fluoride 2 mM (diluted in absolute ethanol), aprotinin 0.1 mg/mL, Triton X-100. The homogenates were centrifuged at 12,000 rpm at 4°C, and the supernatants of each sample were collected. The total protein concentration was determined by the Pierce BCA (Thermo Scientific, Cat. No. 23225) and treated in a Laemmli buffer with 200 mM of dithiothreitol, heated at 100°C for 5 min, and applied in SDS-PAGE gel and transfer to nitrocellulose membrane. The membranes were blocked with 5% of BSA diluted in TBS-T. The primary and secondary antibodies are listed in Supplementary Table. The protein bands were detected using Super Signal West Pico (Thermo Scientific, Cat. No. 34580) in GeneGnome (Syngene), and the band quantification was performed using ImageJ. Statistical analyses were performed using GraphPad Prism, with a significance level set at $p \leq 0.05$. Data are presented as mean ± standard deviation (SD). Normality of the data distribution was assessed using the Shapiro–Wilk test. For datasets following a normal distribution, comparisons were made using the Student t-test. For non-normally distributed data, the Mann–Whitney U test was used. To ensure data transparency, uncropped images showing the full area of all original Western blots presented in this study are available in the Supplementary Material.

## RESULTS

*Coverage and quality of PFC proteome*

Proteomic analysis identified 5,647 protein groups in females and 5,336 in males, corresponding to 70,283 and 67,299 peptides, respectively. Data completeness was 90.60% in females and 96.70% in males, indicating high proteomic coverage in both sexes, with greater completeness in males. The datasets also exhibited high recovery rates (99.70% in females and 99.80% in males) and good quantitative reproducibility, with median coefficients of variation of 27.0% and 19.80%, respectively. Overall, these results demonstrate robust LC-MS/MS performance in both sexes, supporting subsequent differential protein expression and pathway enrichment analyses.

The Spectronaut candidate proteins identified 52 candidates in females (22 up-regulated and 30 down-regulated) and 33 in males (12 up-regulated and 21 down-regulated). Eleven female entries (21%) and five male entries (15%) corresponded to immunoglobulin chains, keratins, MHC class I molecules or unannotated groups; these entries were heterogeneous between sexes (e.g., IGHG3 +819% in females; KRT10 and KRT79 increased in males) and are most likely related to residual blood or handling contamination.

*A sex-opposite CaMKII/IQSEC*

Among parenchymal proteins, only CaMKIIα (Camk2a) and CaMKIIβ (Camk2b) were shared by the female and male candidate lists, and they were regulated in opposite directions: in females, CaMKIIα increased by 69.1% and CaMKIIβ by 52.4% (Figure 1G), whereas in males CaMKIIα decreased by 53.9%, CaMKIIβ by 55.3% and CaMKIIγ by 47.8% (Figure 1H).

Western blot confirmed the direction of change of total CaMKII in both sexes, with an increase in females and a decrease in males (Figure 2). Phosphorylated CaMKII did not differ between groups

in either sex; consequently, the p-CaMKII/CaMKII ratio was reduced in females, indicating that the expanded CaMKII pool was not accompanied by a proportional increase of the phosphorylated fraction, while in males the ratio was unchanged.

*Female-specific candidates*

Besides CaMKII, the female up-regulated candidates included the opioid precursor prodynorphin (Pdyn, +73.6%), neuromedin B (Nmb, +209.9%), caspase-6 (Casp6, +143.5%), cathepsin C (Ctsc, +75.0%), DNA polymerase beta (Polb, +96.7%) and transcriptional machinery components (Taf5l, Polr2l and Ash2l). The down-regulated candidates comprised the peptide shared by the estrogen-related receptors Esrra and Esrrb (-60.8%), the mitochondrial ADP/ATP translocase Slc25a4 (ANT1, -41.7%), the synaptic adhesion protein Flrt1 (-43.4%), the lysosomal enzymes Gla and Naglu, and Stat6, Serping1 and A1bg (Figure 1).

*Male-specific candidates*

In males, besides the CaMKII isoforms and IQSEC1/IQSEC2, the down-regulated candidates included Got2 (-52.2%), Cd81 (-46.3%), Jak1 (-39.0%), Gnb4 (-36.6%), Lcp2 (-67.2%), Sec24d (-55.7%) and Col4a2 (-39.1%). The up-regulated candidates included neurexin-2 (Nrxn2, +120.8%), Pbx3 (+82.6%), the GATOR2 component Wdr24 (+76.0%), Naa38 (+75.0%) and Tmem143 (+143.7%).

*Functional enrichment*

In females, the up-regulated set was enriched in calcium/calmodulin-dependent protein kinase activity (CaMKIIα, CaMKIIβ), neuropeptide hormone activity (PDYN, NMB), regulation of

neuronal synaptic plasticity and dendritic spine development, and in the KEGG pathways amphetamine addiction (CaMKIIα, CaMKIIβ and Pdyn; adjusted P = 0.002), Cushing syndrome and long-term potentiation (Figure 3A). The female down-regulated set was enriched in immunoglobulin complex, Golgi organization, growth hormone receptor signaling (A1bg, Stat6) and ADP transmembrane transporter activity (Slc25a4) (Figure 3B). In males, the down-regulated set was enriched in postsynaptic density and asymmetric synapse (CaMKIIα, β, γ, IQSEC1 and IQSEC2; $q < 0.001$), regulation of protein localization to membrane, calcium/calmodulin-dependent protein kinase activity and the KEGG pathways circadian entrainment, cholinergic and dopaminergic synapse and long-term potentiation (Figure 3D). In the male up-regulated set, cellular component and molecular function terms were driven either by keratins (Krt10 and Krt79) or by single proteins (Naa38, Wdr24, Cenpv and Nrxn2) (Figure 3C); the biological process analysis supplied for this set had been computed on a gene list containing keratins absent from the male candidate list (Krt1, Krt15, Krt77 and Krt78) and was therefore not used. Noticeably, terms such as tuberculosis, necroptosis, interferon gamma signaling and HSF1-dependent transactivation were driven exclusively by CaMKII annotations and do not represent independent biological pathways.

*Cellular context*

In the SCP2126 single-nucleus dataset (mouse cortex, vehicle-treated animals, 134,083 nuclei), Camk2a, Camk2b and Iqsec2 were detected mainly in neurons (CAMK2a in 94.9% of excitatory and 77.8% of inhibitory nuclei), Camk2g also in astrocytes (63.5%), Iqsec1 in neurons and oligodendrocytes (47.7%), and Camk2d was broadly distributed. Got2 was detected mainly in neurons (41.5% and 47.9% of excitatory and inhibitory nuclei). Among female candidates, Ctsc

was enriched in microglia (23.1%) and endothelial cells (15.6%), Casp6 in endothelial cells (7.1%), Pdyn in inhibitory neurons (6.2%) and Polb in neurons (62.7% and 69.7%); among male candidates, Nrxn2 was detected in oligodendrocyte precursor cells (83.1%) and neurons, and Pbx3 in fibroblasts (59.4%) (Figure 4). Thus, the sex-opposite module most likely originates in neurons, whereas part of the female candidates may reflect microglial and vascular compartments. SCP2126 covers the whole mouse cortex rather than the PFC and was not generated in aged or sex-stratified animals, so that these assignments are approximations.

*Western blot of tau and beta amyloid*

Total and phosphorylated tau did not differ between groups in either sex; however, the p-tau/tau ratio was increased in males. (Figure 5).

*Western blot of AKT, IRS and mTOR*

Total IRS-1 did not differ in either sex; phosphorylated IRS-1 was increased in females, whereas in males the p-IRS-1/IRS-1 ratio was increased. Phosphorylated Akt1/2/3 was increased in males only (Figure 6).

**DISCUSSION**

The present study indicates that prenatal unpredictable chronic mild stress (UCMS is associated with sex-dependent alterations in the prefrontal cortex (PFC) proteome of aged mice. The most consistent finding was the opposite regulation of a postsynaptic module comprising CaMKII isoforms in males and females. Additional findings suggest potential alterations in mitochondrial

metabolism and stress-related signaling, while the behavioral results indicate sex-dependent trajectories in the emergence of anhedonia [18].

In aged males, the reduced abundance of CaMKII and IQSEC proteins suggests remodeling of the postsynaptic machinery involved in synaptic organization and plasticity. CaMKII is a major component of the postsynaptic density and plays a central role in synaptic plasticity, learning, and memory, whereas CaMKIIβ contributes to dendritic spine organization through its interaction with F-actin [33–35]. IQSEC1 and IQSEC2 couple glutamate receptor signaling to Arf6-dependent receptor trafficking [36, 37]. Their coordinated reduction is therefore consistent with alterations in excitatory synaptic organization. This interpretation agrees with reports of reduced dendritic complexity and spine density following prenatal or chronic stress, as well as decreased CaMKII abundance after chronic stress and maternal deprivation [22, 24, 38] Furthermore, prenatal psychosocial stress alters calcium-signaling and neurotransmission-related genes in male offspring, with some effects attributable to the postnatal maternal environment [12]. Together, these findings support the possibility that prenatal adversity and subsequent maternal care contribute to long-lasting changes in synaptic organization.

However, stress-related CaMKII responses are not uniform across experimental models. Increased total and phosphorylated CaMKII has been reported in the hippocampus following prenatal restraint stress, while other studies have identified increased excitatory drive after early-life adversity [15, 39, 40]. These discrepancies may reflect differences in brain region, developmental stage, stress paradigm, and compensatory responses. Because the present study examined the PFC at 18 months, its findings may reflect late-life adaptations that differ from those observed in younger animals or in the hippocampus.

In females, the CaMKII/IQSEC showed an opposite abundance pattern, accompanied by a reduced phosphorylated CaMKII-to-total CaMKII ratio. This finding suggests that increased protein abundance does not necessarily correspond to greater kinase activity. CaMKII has both catalytic and structural functions in synaptic organization, and Thr286 autophosphorylation is particularly important for autonomous activity and synaptic potentiation [41–43]. Thus, the female profile may reflect an expansion of the postsynaptic protein pool without a proportional increase in its catalytically active fraction. Sex-dependent regulation of synaptic structure and signaling is biologically plausible, given the effects of gonadal steroids and sex-specific molecular mechanisms on cortical plasticity [22, 23, 44, 45]. However, an estrogen-dependent explanation is less convincing in 18-month-old females, considering reproductive senescence and the limited evidence that local estrogen synthesis can sustain brain function indefinitely [46, 47]. Developmental programming of sex-specific synaptic regulation is therefore an alternative hypothesis, although it remains untested in the present model. Importantly, the female effect was sensitive to the exclusion of an outlying control animal, and only three stressed females were included. The proposed expansion of the CaMKII/IQSEC module should consequently be regarded as provisional. Overall, the opposing patterns suggest sex-dependent postsynaptic remodeling rather than a uniform response to prenatal stress.

Additional candidates related to mitochondrial function, including ESRRA/ESRRB and the ADP/ATP translocase SLC25A4, as well as proteins associated with inflammatory processes, suggest that the phenotype may involve convergent changes in energy metabolism, neuronal function, and cellular stress responses. These interpretations remain exploratory because several candidates were quantified using only one peptide and did not achieve significance in animal-level analyses. The available evidence therefore supports a multifactorial hypothesis rather than a single-

molecule explanation for delayed anhedonia in females. Targeted quantification of dynorphin peptides, assessment of mitochondrial function, and pharmacological manipulation of KOR signaling will be necessary to establish whether these candidates contribute to the observed trajectory.

The reduction in GOT2 provides a potential link between prenatal adversity and altered energy metabolism in aged males. GOT2 participates in the malate–aspartate shuttle and in aspartate and glutamate metabolism, connecting mitochondrial redox balance with cellular metabolic function. Its reduced abundance is consistent with the possibility of compromised metabolic support, although enzyme activity and mitochondrial function were not directly measured. Western blot findings involving insulin signaling and tau phosphorylation also require cautious interpretation. Increased basal Akt phosphorylation does not, by itself, establish insulin resistance, which is defined by an attenuated response to insulin stimulation. Moreover, because Akt can inhibit GSK3β, the simultaneous increase in phosphorylated Akt and phosphorylated tau cannot be mechanistically resolved without information about the phosphorylation sites, quantitative effect sizes, and responses to insulin stimulation [48–50]. Accordingly, the present results neither confirm nor exclude impaired insulin signaling. GOT2 remains a candidate marker of metabolic remodeling, whereas the proposed relationship among insulin resistance, Akt signaling, and tau phosphorylation requires further investigation. The observed increase in neurexin-2 is also hypothesis-generating but lacks sufficient statistical support for mechanistic conclusions.

Previous proteomic investigations of prenatal and chronic stress have identified alterations in synaptic, cytoskeletal, membrane-trafficking, and metabolic proteins, with outcomes varying according to sex, brain region, and susceptibility phenotype [25, 26, 51].

In conclusion, prenatal UCMS was associated with sex-dependent proteomic changes in the aged PFC. The most consistent candidate signature involved opposite regulation of the postsynaptic CaMKII/IQSEC module in males and females, potentially reflecting distinct forms of synaptic remodeling. The behavioral findings further suggest that anhedonia may emerge at different ages across sexes. Given the limited sample size and absence of proteome-wide significant individual proteins, these findings should be interpreted as hypothesis-generating. Independent validation and longitudinal, region-specific analyses are essential to determine whether these molecular signatures contribute to sex-dependent trajectories of brain aging following prenatal adversity.

## Statements & Declarations

**Funding.** This research was partially funded by the Coordenação de Aperfeiçoamento de Pessoal de Nível Superior (CAPES), the National Council for Scientific and Technological Development (CNPq) [308043/2022-7], the Brazilian National Institute of Science and Technology of DOHaD-INCT [409165/2024-7] and the São Paulo Research Foundation (FAPESP) [2024/06071-1 and 2025/14634-9].

**Declaration of competing interest.** The authors declare no competing interests.

**Author Contributions.** Material preparation, data collection and analysis were performed by Bruno Calsa, Amanda Cristina de Souza, Luiz Marcos Frediani Portela, Gabriel Boer Grigoletti-Lima. The first draft of the manuscript was written by Bruno Calsa and Gabriel Boer Grigoletti-Lima and all authors commented on previous versions of the manuscript. All authors read and approved the final manuscript.

**Data Availability.** The datasets generated during and/or analysed during the current study are available within the article and its supplementary materials.

**Declaration of generative AI and AI-assisted technologies in the manuscript preparation process.** During the preparation of this work the authors used Claude (Anthropic) to re-analyze the exported proteomic matrices, to perform the false discovery rate, interaction and module analyses, to generate draft figures and to draft the text. After using this tool, the authors reviewed and edited the content as needed and take full responsibility for the content of the published article.

## REFERENCES


1. Weinstock M (2017) Prenatal stressors in rodents: effects on behavior. Neurobiol Stress 6:3–13. https://doi.org/10.1016/j.ynstr.2016.08.004
2. Bale TL, Epperson CN (2015) Sex differences and stress across the lifespan. Nat Neurosci 18:1413–1420. https://doi.org/10.1038/nn.4112
3. Mueller BR, Bale TL (2008) Sex-specific programming of offspring emotionality after stress early in pregnancy. Journal of Neuroscience 28:9055–9065. https://doi.org/10.1523/JNEUROSCI.1424-08.2008
4. Bale TL (2016) The placenta and neurodevelopment: sex differences in prenatal vulnerability. Dialogues Clin Neurosci 18:459–464. https://doi.org/10.31887/DCNS.2016.18.4/tbale
5. Van den Hove DL, Kenis G, Brass A, et al (2013) Vulnerability versus resilience to prenatal stress in male and female rats; implications from gene expression profiles in the hippocampus and frontal cortex. European Neuropsychopharmacology 23:1226–1246. https://doi.org/10.1016/j.euroneuro.2012.09.011
6. Shoshani-Haye K, Friedlander G, Golani O, et al (2025) Prenatal stress induces transient developmental alterations in distinct GABAergic populations and leads to long-lasting

behavioral abnormalities. Neurobiol Stress 38:100749. https://doi.org/10.1016/j.ynstr.2025.100749

7. Bowman RE, MacLusky NJ, Sarmiento Y, et al (2004) Sexually dimorphic effects of prenatal stress on cognition, hormonal responses, and central neurotransmitters. Endocrinology 145:3778–3787. https://doi.org/10.1210/en.2003-1759
8. Bowman RE (2005) Stress-induced changes in spatial memory are sexually differentiated and vary across the lifespan. J Neuroendocrinol 17:526–535. https://doi.org/10.1111/j.1365-2826.2005.01335.x
9. Luine VN, Beck KD, Bowman RE, et al (2007) Chronic stress and neural function: accounting for sex and age. J Neuroendocrinol 19:743–751. https://doi.org/10.1111/j.1365-2826.2007.01594.x
10. Cao Z, Zhang X, Gao F, et al (2025) Double-hit of MIA and Nod2 deficiency induces sex-specific offspring behavioral abnormalities through placental dysregulation. Transl Psychiatry 15:527. https://doi.org/10.1038/s41398-025-03747-z
11. Musillo C, Ajmone-Cat MA, De Simone R, et al (2025) Maternal stressors disrupt mouse placental proteome and fetal brain development in a sex-specific fashion through inflammation and oxidative stress. Mol Psychiatry 30:5072–5083. https://doi.org/10.1038/s41380-025-03090-1
12. Zoubovsky SP, Williams MT, Hoseus S, et al (2022) Neurobehavioral abnormalities following prenatal psychosocial stress are differentially modulated by maternal environment. Transl Psychiatry 12:22. https://doi.org/10.1038/s41398-022-01785-5

13. Baram TZ, Davis EP, Obenaus A, et al (2012) Fragmentation and unpredictability of early-life experience in mental disorders. American Journal of Psychiatry 169:907–915. https://doi.org/10.1176/appi.ajp.2012.11091347

14. Molet J, Heins K, Zhuo X, et al (2016) Fragmentation and high entropy of neonatal experience predict adolescent emotional outcome. Transl Psychiatry 6:e702. https://doi.org/10.1038/tp.2015.200

15. Creutzberg KC, Begni V, Orso R, et al (2023) Vulnerability and resilience to prenatal stress exposure: behavioral and molecular characterization in adolescent rats. Transl Psychiatry 13:358. https://doi.org/10.1038/s41398-023-02653-6

16. Vall{'{e}}e M, Maccari S, Dellu F, et al (1999) Long-term effects of prenatal stress and postnatal handling on age-related glucocorticoid secretion and cognitive performance: a longitudinal study in the rat. European Journal of Neuroscience 11:2906–2916. https://doi.org/10.1046/j.1460-9568.1999.00705.x

17. Morelli G, Visintin G, Gelli E, et al (2026) Traumatic life experiences during critical periods lead to diverse developmental trajectories. Cell Rep Med 7:102798. https://doi.org/10.1016/j.xcrm.2026.102798

18. Souza AC, Mariano VS, Tibiri{\c{c}}{'{a}} ICG, et al (2026) Early-life stress induces sexually dimorphic brain aging via mesolimbic alterations and fronto-striatal dysfunction. Submitted. https://doi.org/10.64898/2026.10.09.757621

19. McEwen BS, Morrison JH (2013) The brain on stress: vulnerability and plasticity of the prefrontal cortex over the life course. Neuron 79:16–29. https://doi.org/10.1016/j.neuron.2013.06.028

20. Holmes A, Wellman CL (2009) Stress-induced prefrontal reorganization and executive dysfunction in rodents. Neurosci Biobehav Rev 33:773–783. https://doi.org/10.1016/j.neubiorev.2008.11.005

21. Morrison JH, Baxter MG (2012) The ageing cortical synapse: hallmarks and implications for cognitive decline. Nat Rev Neurosci 13:240–250. https://doi.org/10.1038/nrn3200

22. Garrett JE, Wellman CL (2009) Chronic stress effects on dendritic morphology in medial prefrontal cortex: sex differences and estrogen dependence. Neuroscience 162:195–207. https://doi.org/10.1016/j.neuroscience.2009.04.057

23. Shansky RM, Hamo C, Hof PR, et al (2010) Estrogen promotes stress sensitivity in a prefrontal cortex-amygdala pathway. Cerebral Cortex 20:2560–2567. https://doi.org/10.1093/cercor/bhq003

24. Murmu MS, Salomon S, Biala Y, et al (2006) Changes of spine density and dendritic complexity in the prefrontal cortex in offspring of mothers exposed to stress during pregnancy. European Journal of Neuroscience 24:1477–1487. https://doi.org/10.1111/j.1460-9568.2006.05024.x

25. Liao W, Liu Y, Wang L, et al (2021) Chronic mild stress-induced protein dysregulations correlated with susceptibility and resiliency to depression or anxiety revealed by quantitative proteomics of the rat prefrontal cortex. Transl Psychiatry 11:143. https://doi.org/10.1038/s41398-021-01267-0

26. He W, Huang H, Zhang H, Sun H (2022) Comparative phosphoproteomic profiling in the prefrontal cortex of prenatally stressed male offspring rats. Dev Neurosci 44:532–546. https://doi.org/10.1159/000525801

27. Wi{'{s}}niewski JR, Zougman A, Nagaraj N, Mann M (2009) Universal sample preparation method for proteome analysis. Nat Methods 6:359–362. https://doi.org/10.1038/nmeth.1322

28. Bruderer R, Bernhardt OM, Gandhi T, et al (2015) Extending the limits of quantitative proteome profiling with data-independent acquisition and application to acetaminophen-treated three-dimensional liver microtissues. Molecular \& Cellular Proteomics 14:1400–1410. https://doi.org/10.1074/mcp.M114.044305

29. Storey JD, Tibshirani R (2003) Statistical significance for genomewide studies. Proceedings of the National Academy of Sciences of the USA 100:9440–9445. https://doi.org/10.1073/pnas.1530509100

30. Wu T, Hu E, Xu S, et al (2021) clusterProfiler 4.0: a universal enrichment tool for interpreting omics data. The Innovation 2:100141. https://doi.org/10.1016/j.xinn.2021.100141

31. Yu G, He QY (2016) ReactomePA: an R/Bioconductor package for reactome pathway analysis and visualization. Mol Biosyst 12:477–479. https://doi.org/10.1039/c5mb00663e

32. Mortberg MA, Gentile JE, Nadaf NM, et al (2023) A single-cell map of antisense oligonucleotide activity in the brain. Nucleic Acids Res 51:7109–7124. https://doi.org/10.1093/nar/gkad371

33. Lisman J, Schulman H, Cline H (2002) The molecular basis of CaMKII function in synaptic and behavioural memory. Nat Rev Neurosci 3:175–190. https://doi.org/10.1038/nrn753

34. Shen K, Teruel MN, Subramanian K, Meyer T (1998) CaMKII$eta$ functions as an F-actin targeting module that localizes CaMKII$lpha/eta$ heterooligomers to dendritic spines. Neuron 21:593–606. https://doi.org/10.1016/s0896-6273(00)80569-3

35. Yasuda R, Hayashi Y, Hell JW (2022) CaMKII: a central molecular organizer of synaptic plasticity, learning and memory. Nat Rev Neurosci 23:666–682. https://doi.org/10.1038/s41583-022-00624-2

36. Scholz R, Berberich S, Rathgeber L, et al (2010) AMPA receptor signaling through BRAG2 and Arf6 critical for long-term synaptic depression. Neuron 66:768–780. https://doi.org/10.1016/j.neuron.2010.05.003

37. Elagabani MN, Bri{ {s}}evac D, Kintscher M, et al (2016) Subunit-selective N-methyl-D-aspartate (NMDA) receptor signaling through brefeldin A-resistant Arf guanine nucleotide exchange factors BRAG1 and BRAG2 during synapse maturation. Journal of Biological Chemistry 291:9105–9118. https://doi.org/10.1074/jbc.M115.691717

38. Gerges NZ, Aleisa AM, Schwarz LA, Alkadhi KA (2004) Reduced basal CaMKII levels in hippocampal CA1 region: possible cause of stress-induced impairment of LTP in chronically stressed rats. Hippocampus 14:402–410. https://doi.org/10.1002/hipo.10193

39. Cai Q, Zhang B, Huang S, et al (2011) The effects of prenatal stress on expression of CaMK-II and L-Ca2+ channel in offspring hippocampus. Acta Biochim Biophys Sin (Shanghai) 43:601–606. https://doi.org/10.1093/abbs/gmr057

40. Biro L, Miskolczi C, Szebik H, et al (2023) Post-weaning social isolation in male mice leads to abnormal aggression and disrupted network organization in the prefrontal cortex: contribution of parvalbumin interneurons with or without perineuronal nets. Neurobiol Stress 25:100546. https://doi.org/10.1016/j.ynstr.2023.100546

41. Giese KP, Fedorov NB, Filipkowski RK, Silva AJ (1998) Autophosphorylation at threonine 286 of the alpha calcium-calmodulin kinase II in LTP and learning. Science (1979) 279:870–873. https://doi.org/10.1126/science.279.5352.870

42. Chang JY, Parra-Bueno P, Laviv T, et al (2017) CaMKII autophosphorylation is necessary for optimal integration of Ca2+ signals during LTP induction, but not maintenance. Neuron 94:800-808.e4. https://doi.org/10.1016/j.neuron.2017.04.041

43. Bayer KU, Giese KP (2025) A revised view of the role of CaMKII in learning and memory. Nat Neurosci 28:24–34. https://doi.org/10.1038/s41593-024-01809-x

44. Hara Y, Waters EM, McEwen BS, Morrison JH (2015) Estrogen effects on cognitive and synaptic health over the lifecourse. Physiol Rev 95:785–807. https://doi.org/10.1152/physrev.00036.2014

45. Jain A, Huang GZ, Woolley CS (2019) Latent sex differences in molecular signaling that underlies excitatory synaptic potentiation in the hippocampus. Journal of Neuroscience 39:1552–1565. https://doi.org/10.1523/JNEUROSCI.1897-18.2018

46. Felicio LS, Nelson JF, Finch CE (1984) Longitudinal studies of estrous cyclicity in aging C57BL/6J mice: II. Cessation of cyclicity and the duration of persistent vaginal cornification. Biol Reprod 31:446–453. https://doi.org/10.1095/biolreprod31.3.446

47. Flannery JC, Tirrell PS, Baumgartner NE, Daniel JM (2025) Neuroestrogens, the hippocampus, and female cognitive aging. Horm Behav 170:105710. https://doi.org/10.1016/j.yhbeh.2025.105710

48. Hooper C, Killick R, Lovestone S (2008) The GSK3 hypothesis of Alzheimer's disease. J Neurochem 104:1433–1439. https://doi.org/10.1111/j.1471-4159.2007.05194.x

49. Grillo CA, Piroli GG, Lawrence RC, et al (2015) Hippocampal insulin resistance impairs spatial learning and synaptic plasticity. Diabetes 64:3927–3936. https://doi.org/10.2337/db15-0596

50. Grillo CA, Woodruff JL, Macht VA, Reagan LP (2019) Insulin resistance and hippocampal dysfunction: disentangling peripheral and brain causes from consequences. Exp Neurol 318:71–77. https://doi.org/10.1016/j.expneurol.2019.04.012

51. F{"{o}}cking M, Opstelten R, Prickaerts J, et al (2014) Proteomic investigation of the hippocampus in prenatally stressed mice implicates changes in membrane trafficking, cytoskeletal, and metabolic function. Dev Neurosci 36:432–442. https://doi.org/10.1159/000365327

## FIGURES, TABLES AND SUPPLEMENTARY FILE LEGENDS

**Figure 1:** Proteomic overview and candidate proteins in the prefrontal cortex of 18-month-old offspring following prenatal stress. (A, D) Principal component analysis of the complete proteomic datasets. (B, E) Volcano plots showing significance versus fold change at the individual animal level. Highlighted are the CaMKII/IQSEC module and key candidates. (C, F) Distribution of animal-level P values indicating overall proteomic variance. (G, H) Differentially abundant protein candidates ranked by log2 fold change, distinguishing those meeting statistical significance across experimental groups for females and males, respectively. C: Control, S: Prenatal Stress.

**Figure 2:** Validation of CaMKII abundance and phosphorylation by Western blot. Total and phosphorylated levels (Thr286) of CaMKII were evaluated across control (C) and stressed (S) offspring in both females (F) and males (M). Bar charts demonstrate log2 quantifications and relative expression normalized to α-Tubulin (A-F), and the ratio of p-CaMKII to total CaMKII (G). Representative Western blot images are shown in (H). Error bars represent mean ± SD.

**Figure 3:** Functional enrichment analysis of differentially abundant proteins in the prefrontal cortex. Sankey diagrams illustrating significant Gene Ontology biological processes, cellular components, molecular functions, and KEGG pathways enriched in up-regulated (Up) and down-regulated (Down) candidate proteins for females (A) and males (B).

**Figure 4:** Cell-type expression mapping of candidate proteins. Normalized mean expression of selected candidate genes and the CaMKII/IQSEC module in distinct brain cell populations, derived from the SCP2126 mouse cortex single-nucleus RNA-sequencing dataset. Dot size represents the percentage of nuclei expressing each gene.

**Figure 5:** Assessment of Tau phosphorylation and beta-amyloid levels. Protein levels of total TAU (A), phosphorylated TAU at Ser199/202 (B), ratio of pTAU/TAU (C), and beta-amyloid (D)

measured in control (C) and stressed (S) female (F) and male (M) groups. Representative immunoblots normalized to α-Tubulin (E). Error bars represent mean ± SD.

**Figure 6:** Assessment of insulin signaling pathway components. Relative expression of total and phosphorylated forms of IRS-1 (A, B) and their ratio (C), mTOR (D, E) and its ratio (F), and phosphorylated AKT1/2/3 (G). Representative Western blots for all targets normalized to α-Tubulin are shown in (H).

**Table 1:** Design, quality metrics and statistical overview of the PFC proteomes of 18-month-old offspring**.**

**Table 2:** Selected parenchymal candidates in the PFC of 18-month-old prenatally stressed offspring, with candidates and animal-level statistics.

**File S1:** Antibodies used in Western blot experiment.

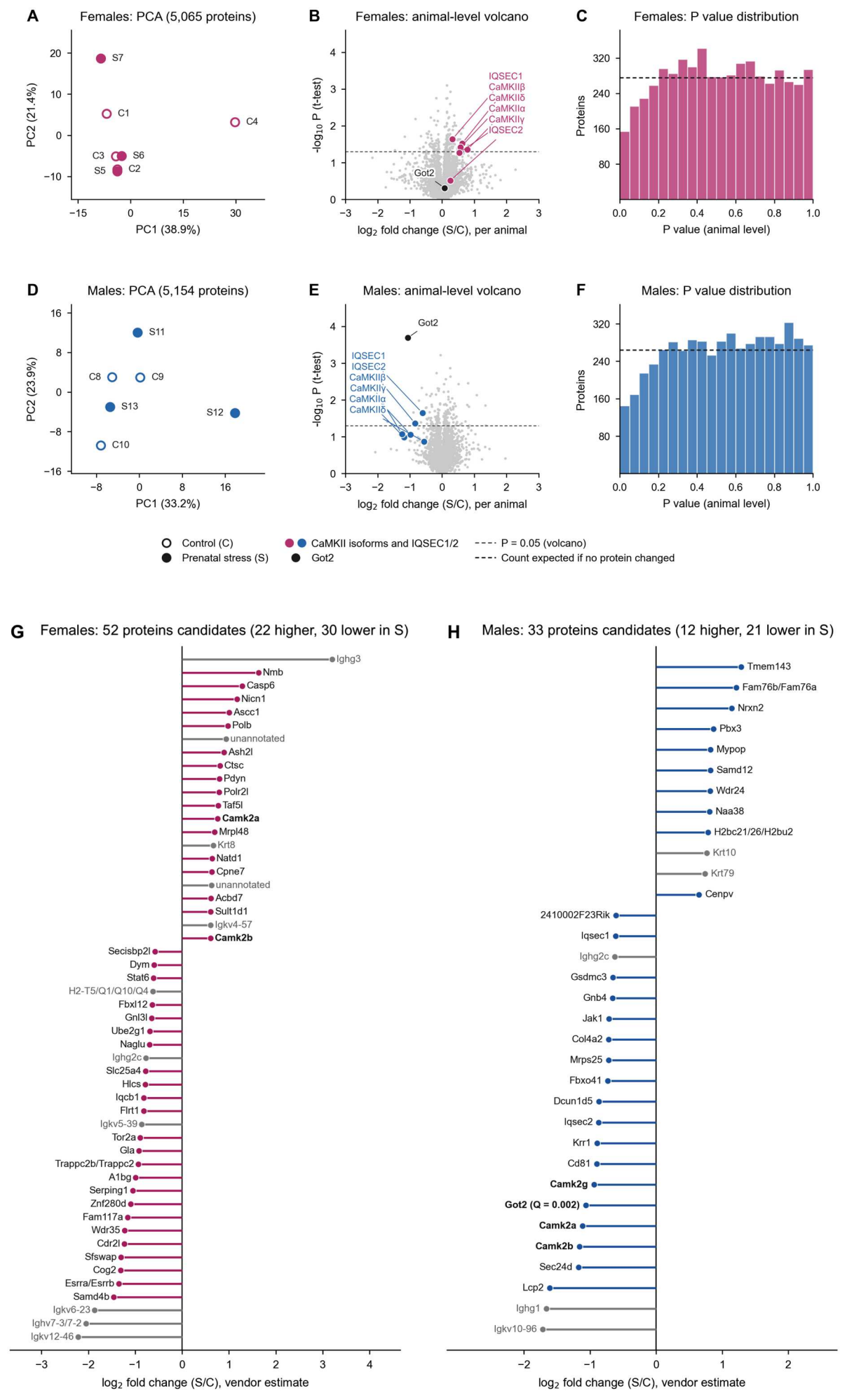
**File S2:** Spectronaut of females dataset.

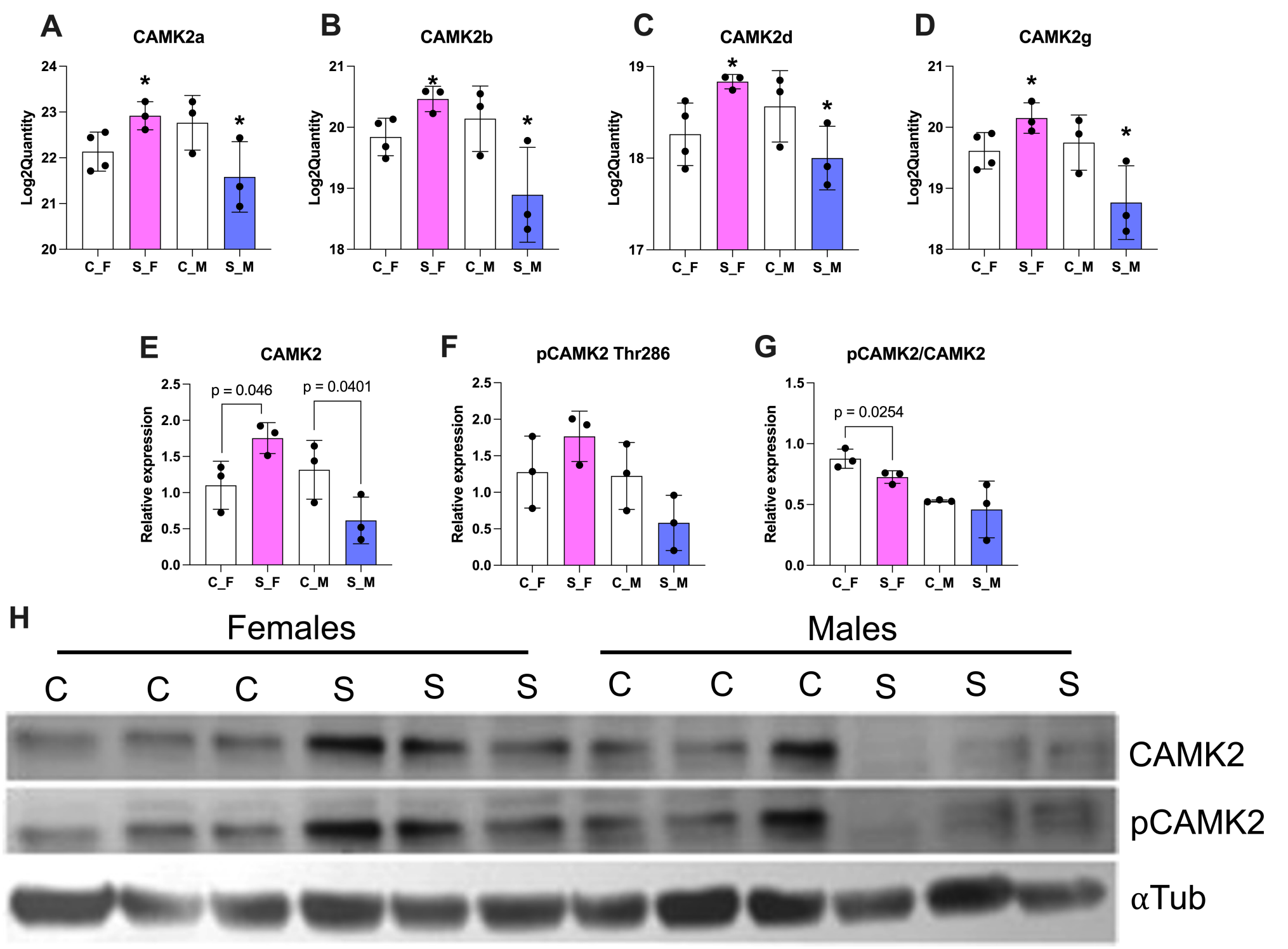
**File S3:** Spectronaut of males dataset.

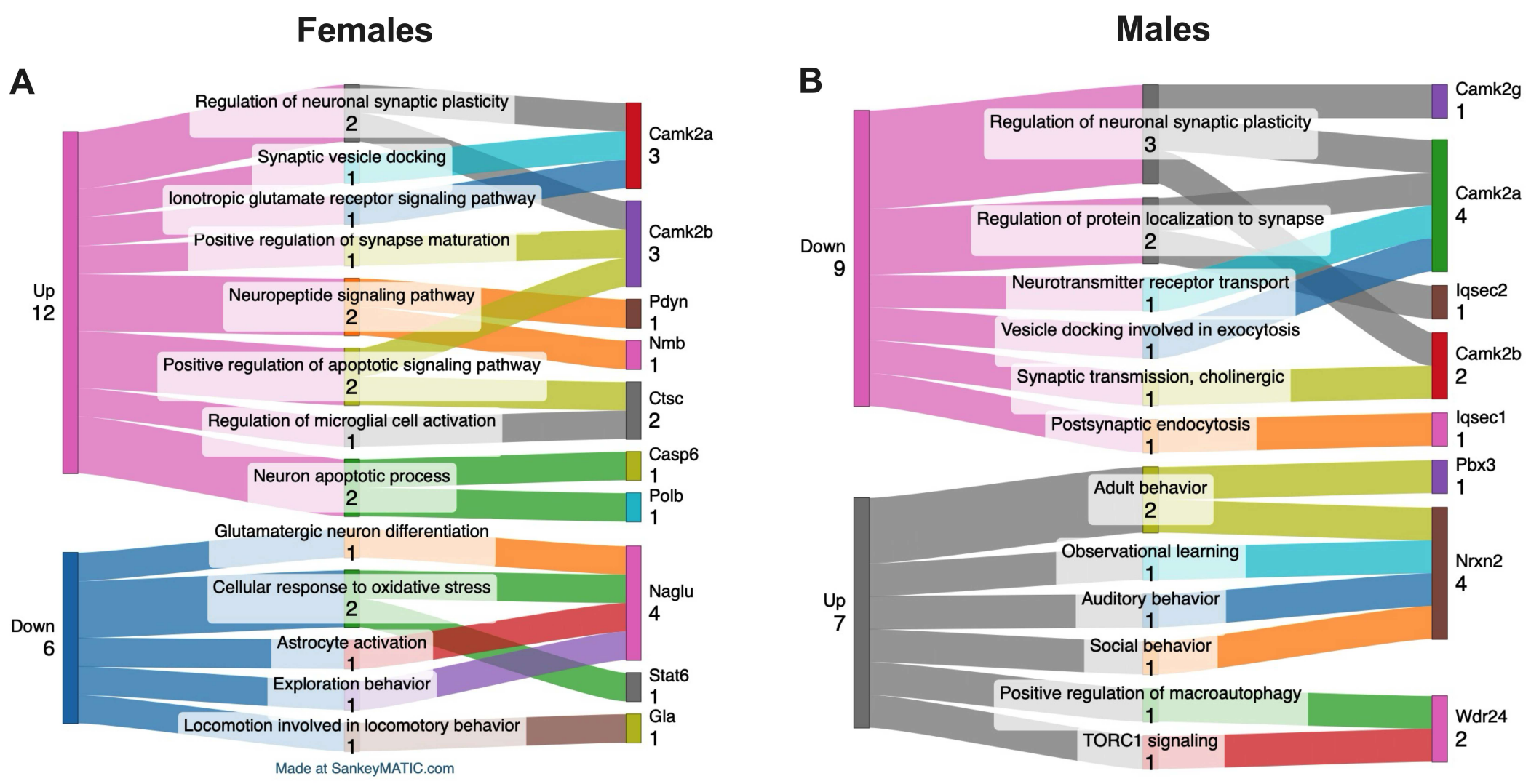
**File S4:** Enrichment tables of female dataset.

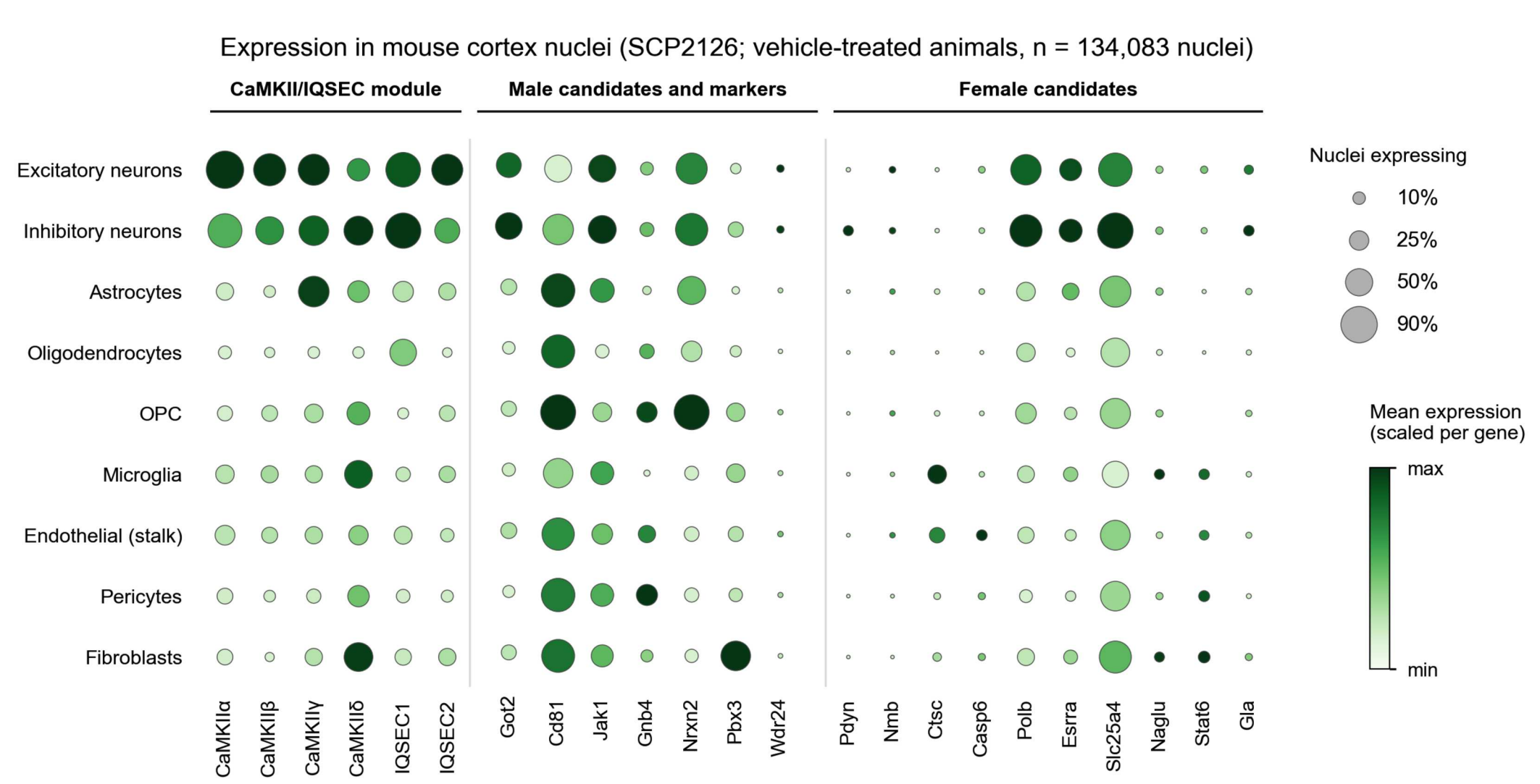
**File S5:** Enrichment tables of female dataset.

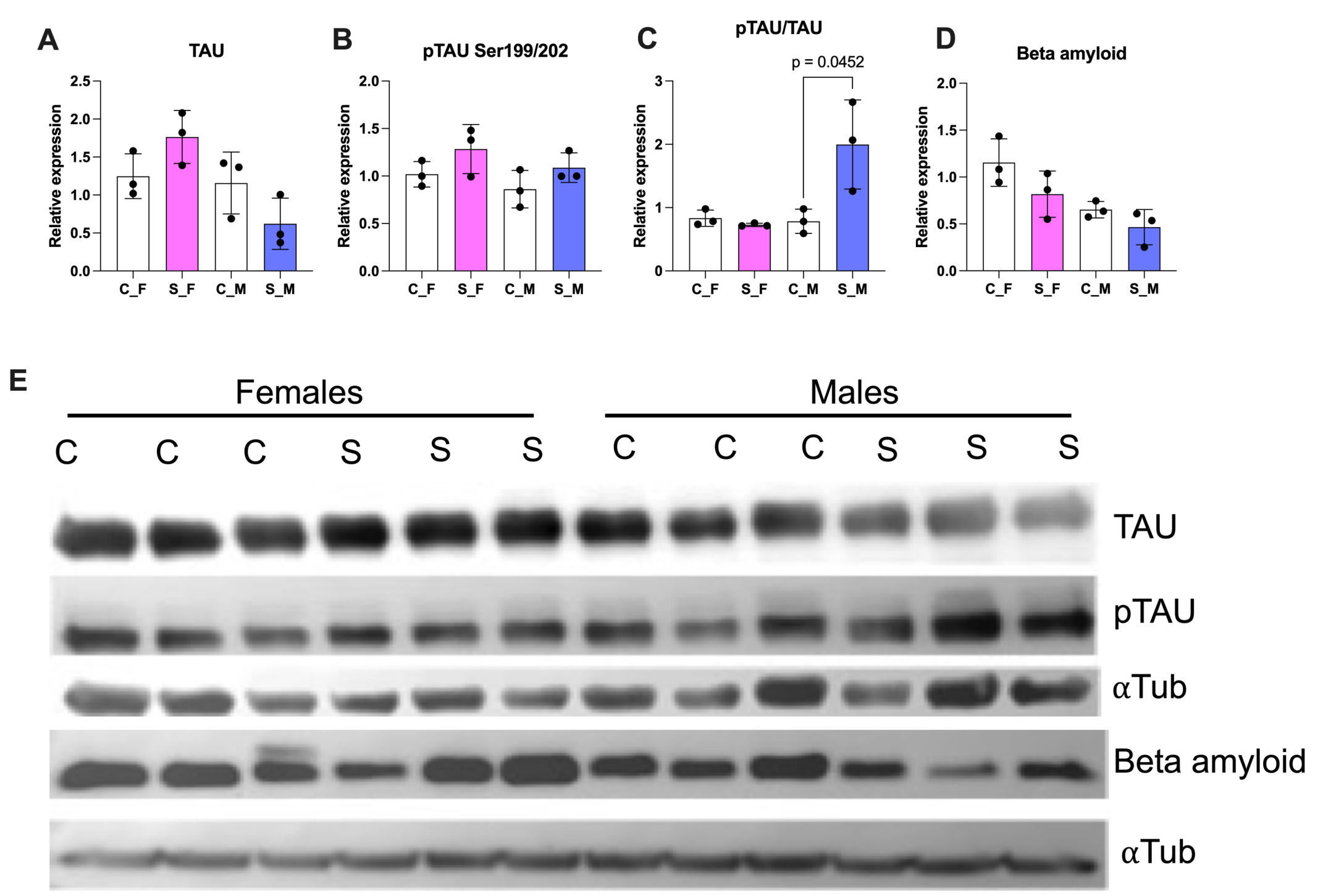
**File S6:** Original, uncropped blot images.

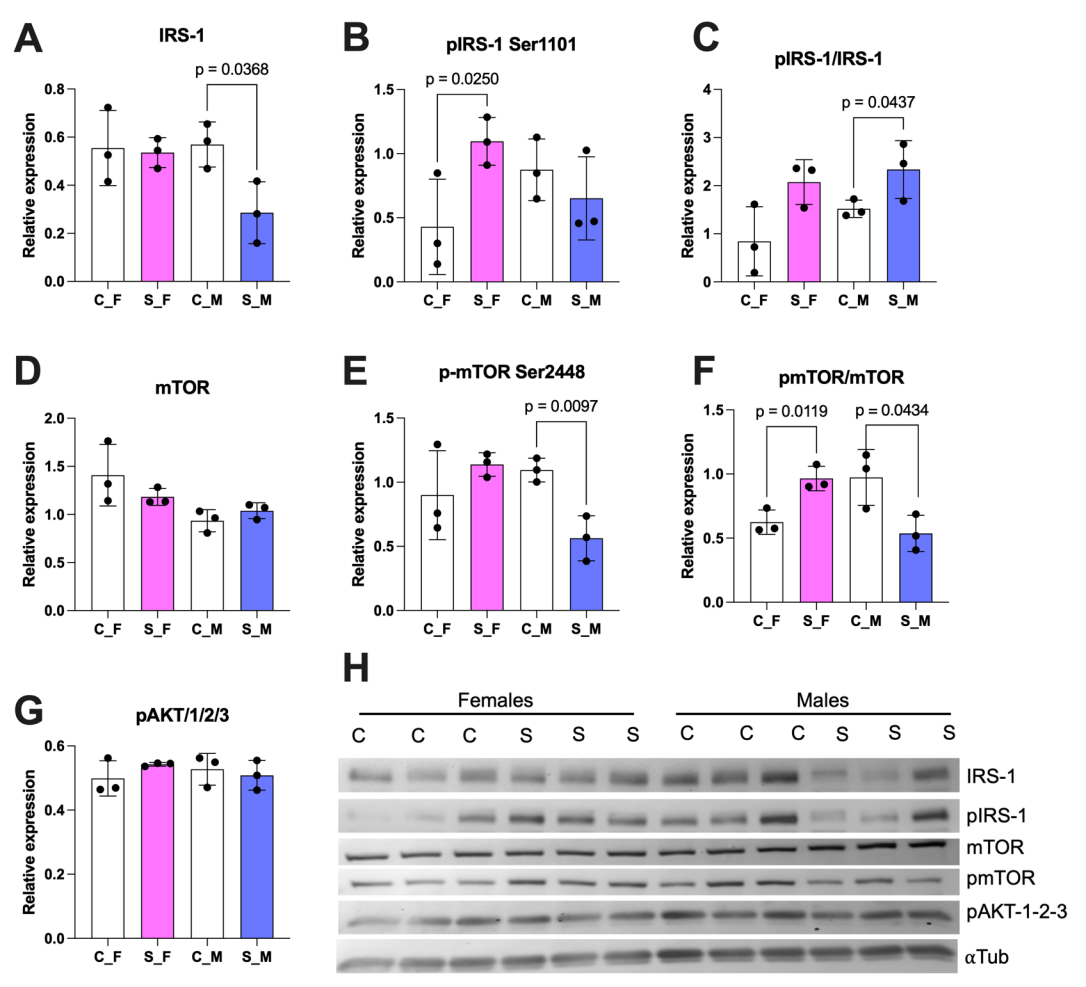

A
Females: PCA (5,065 proteins)
PC2 (21.4%)
PC1 (38.9%)
S7
C1
C4
C3
S6
S5
C2
B
Females: animal-level volcano
-log10 P (t-test)
log2 fold change (S/C), per animal
IQSEC1
CaMKIIβ
CaMKIIδ
CaMKIIα
CaMKIIγ
IQSEC2
Got2
C
Females: P value distribution
Proteins
P value (animal level)
D
Males: PCA (5,154 proteins)
PC2 (23.9%)
PC1 (33.2%)
S11
C8
C9
S13
S12
C10
E
Males: animal-level volcano
-log10 P (t-test)
log2 fold change (S/C), per animal
Got2
IQSEC1
IQSEC2
CaMKIIβ
CaMKIIγ
CaMKIIα
CaMKIIδ
F
Males: P value distribution
Proteins
P value (animal level)
Control (C)
Prenatal stress (S)
CaMKII isoforms and IQSEC1/2
Got2
P = 0.05 (volcano)
Count expected if no protein changed
G
Females: 52 proteins candidates (22 higher, 30 lower in S)
Ighg3
Nmb
Casp6
Nicn1
Ascc1
Polb
unannotated
Ash2l
Ctsc
Pdyn
Polr2l
Taf5l
Camk2a
Mrpl48
Krt8
Natd1
Cpne7
unannotated
Acbd7
Sult1d1
Igkv4-57
Camk2b
Secisbp2l
Dym
Stat6
H2-T5/Q1/Q10/Q4
Fbxl12
Gnl3l
Ube2g1
Naglu
Ighg2c
Slc25a4
Hlcs
Iqcb1
Flrt1
Igkv5-39
Tor2a
Gla
Trappc2b/Trappc2
A1bg
Serping1
Znf280d
Fam117a
Wdr35
Cdr2l
Sfswap
Cog2
Esrra/Esrrb
Samd4b
Igkv6-23
Ighv7-3/7-2
Igkv12-46
log2 fold change (S/C), vendor estimate
H
Males: 33 proteins candidates (12 higher, 21 lower in S)
Tmem143
Fam76b/Fam76a
Nrxn2
Pbx3
Mypop
Samd12
Wdr24
Naa38
H2bc21/26/H2bu2
Krt10
Krt79
Cenpv
2410002F23Rik
Iqsec1
Ighg2c
Gsdmc3
Gnb4
Jak1
Col4a2
Mrps25
Fbxo41
Dcun1d5
Iqsec2
Krr1
Cd81
Camk2g
Got2 (Q = 0.002)
Camk2a
Camk2b
Sec24d
Lcp2
Ighg1
Igkv10-96
log2 fold change (S/C), vendor estimate
Female candidate
Male candidate
Probable non-parenchymal or unannotated entry (immunoglobulin, keratin, MHC-I)


A
CAMK2a
Log2Quantity
24
23
22
21
20
C_F
S_F
C_M
S_M
B
CAMK2b
Log2Quantity
21
20
19
18
C_F
S_F
C_M
S_M
C
CAMK2d
Log2Quantity
19
18
17
C_F
S_F
C_M
S_M
D
CAMK2g
Log2Quantity
21
20
19
18
C_F
S_F
C_M
S_M
E
CAMK2
Relative expression
p = 0.046
p = 0.0401
2.5
2.0
1.5
1.0
0.5
0.0
C_F
S_F
C_M
S_M
F
pCAMK2 Thr286
Relative expression
2.5
2.0
1.5
1.0
0.5
0.0
C_F
S_F
C_M
S_M
G
pCAMK2/CAMK2
Relative expression
p = 0.0254
1.5
1.0
0.5
0.0
C_F
S_F
C_M
S_M
H
Females
Males
C
C
C
S
S
S
C
C
C
S
S
S
CAMK2
pCAMK2
αTub


Females
A
Regulation of neuronal synaptic plasticity
2
Synaptic vesicle docking
1
Ionotropic glutamate receptor signaling pathway
1
Positive regulation of synapse maturation
1
Neuropeptide signaling pathway
2
Positive regulation of apoptotic signaling pathway
2
Regulation of microglial cell activation
1
Neuron apoptotic process
2
Glutamatergic neuron differentiation
1
Cellular response to oxidative stress
2
Astrocyte activation
1
Exploration behavior
1
Locomotion involved in locomotory behavior
1
Up
12
Down
6
Camk2a
3
Camk2b
3
Pdyn
1
Nmb
1
Ctsc
2
Casp6
1
Polb
1
Naglu
4
Stat6
1
Gla
1
Made at SankeyMATIC.com
Males
B
Regulation of neuronal synaptic plasticity
3
Regulation of protein localization to synapse
2
Neurotransmitter receptor transport
1
Vesicle docking involved in exocytosis
1
Synaptic transmission, cholinergic
1
Postsynaptic endocytosis
1
Adult behavior
2
Observational learning
1
Auditory behavior
1
Social behavior
1
Positive regulation of macroautophagy
1
TORC1 signaling
1
Down
9
Up
7
Camk2g
1
Camk2a
4
Iqsec2
1
Camk2b
2
Iqsec1
1
Pbx3
1
Nrxn2
4
Wdr24
2


Expression in mouse cortex nuclei (SCP2126; vehicle-treated animals, n = 134,083 nuclei)
CaMKII/IQSEC module
Male candidates and markers
Female candidates
Excitatory neurons
Inhibitory neurons
Astrocytes
Oligodendrocytes
OPC
Microglia
Endothelial (stalk)
Pericytes
Fibroblasts
CaMKIIα
CaMKIIβ
CaMKIIγ
CaMKIIδ
IQSEC1
IQSEC2
Got2
Cd81
Jak1
Gnb4
Nrxn2
Pbx3
Wdr24
Pdyn
Nmb
Ctsc
Casp6
Polb
Esrra
Slc25a4
Naglu
Stat6
Gla
Nuclei expressing
10%
25%
50%
90%
Mean expression
(scaled per gene)
max
min


A
TAU
Relative expression
2.5
2.0
1.5
1.0
0.5
0.0
C_F
S_F
C_M
S_M
B
pTAU Ser199/202
Relative expression
2.0
1.5
1.0
0.5
0.0
C_F
S_F
C_M
S_M
C
pTAU/TAU
p = 0.0452
Relative expression
3
2
1
0
C_F
S_F
C_M
S_M
D
Beta amyloid
Relative expression
2.0
1.5
1.0
0.5
0.0
C_F
S_F
C_M
S_M
E
Females
Males
C C C S S S C C C S S S
TAU
pTAU
αTub
Beta amyloid
αTub


A
IRS-1
p = 0.0368
Relative expression
C_F
S_F
C_M
S_M
B
pIRS-1 Ser1101
p = 0.0250
C
pIRS-1/IRS-1
p = 0.0437
D
mTOR
E
p-mTOR Ser2448
p = 0.0097
F
pmTOR/mTOR
p = 0.0119
p = 0.0434
G
pAKT/1/2/3
H
Females
Males
C C C S S S C C C S S S
IRS-1
pIRS-1
mTOR
pmTOR
pAKT-1-2-3
αTub

## Supplementary Files

This is a list of supplementary files associated with this preprint. Click to download.

- Table1.docx
- Table2.docx
- FileS1.pdf
- FileS4.pdf
- FileS2.xlsx
- FileS3.xlsx
- FileS5.pdf
- FileS6.pdf